A locally tuned C_{phyto} algorithm for the Ross Sea, Antarctica

Meredith G. Meyer[1] and Walker O. Smith Jr.[2,3]

[1]Department of Earth, Marine, and Environmental Sciences, University of North Carolina at Chapel Hill, Chapel Hill, NC, USA
[2]Virginia Institute of Marine Science, William & Mary, Williamsburg, VA, USA
[3]School of Oceanography, Shanghai Jiao Tong University, Shanghai China

December 13, 2023

Submitted to Geophysical Research Letters
Current publication units: 11.27

Abstract

To improve current estimates of phytoplankton specific carbon in the Ross Sea, we calculated a regionally specific algorithm from in situ particulate organic carbon (POC) concentrations and backscatter sensor data. These data come from three independent Seaglider deployments during the austral summer. Algal-specific POC (C_{phyto}) accounted for between 19.8-61.0% of total POC in the Ross Sea with an average C_{phyto} concentration of 84.2 µg C L^{-1}. As a result, C_{phyto}:chlorophyll *a* ratios were less than POC:chlorophyll *a* ratios and ranged from 9.00-257 µg C (µg chlorophyll *a*) L^{-1}. This regionally-specific method is substantially more accurate (average C_{phyto} concentrations are 10-78 µg C L^{-1} greater) than estimates derived from published algorithms. Our findings highlight the value of regionally-specific algorithms for measuring inherent optical properties and how such approaches can inform our current understanding of particulate carbon partitioning and food web dynamics.

Plain Language Summary

Phytoplankton account for a substantial portion of the organic carbon in the ocean, but not all of it, and traditional sampling methods cannot differentiate between phytoplankton (algal) carbon and non-algal carbon. This frequently leads to overestimates of the amount of algal carbon within an ecosystem. New methods have been developed to measure algal carbon alone, but they are calibrated to the global ocean, making them inaccurate in some regions with specific ecosystem characteristics. Here, we modify one of those methods for the Ross Sea, Antarctica, thus improving its accuracy substantially. Our method shows the importance of developing region specific algorithms in order to develop a better understanding of carbon dynamics, globally.

Key Points

1. When applied to data from the Ross Sea, current algorithms substantially underestimate phytoplankton carbon (C_{phyto}).
2. By modifying pre-existing algorithms with regionally specific data, we can develop regional algorithms to improve our estimates immensely.
3. Our method has potential to substantially improve satellite estimates of Cphyto in regions that have been traditionally difficult to measure.

I. Introduction

Labor-intensive methods and substantial differences among species have made accurate measurements for phytoplankton-specific carbon on large scales a consistent and elusive problem in oceanography for decades. Without this parameter, the accuracy of carbon export, food web, and biogeochemical models remain constrained. Traditional proxies for phytoplankton biomass include chlorophyll *a* (Chl *a*) and particulate organic carbon (POC) concentrations. However, both of these are influenced by factors independent of changes in phytoplankton biomass, specifically phytoplankton physiology (variable chlorophyll *a* concentrations per cell) and detrital carbon stocks (POC), making a quantitative assessment of phytoplankton carbon uncertain.

The development of direct estimates of phytoplankton carbon (C_{phyto}) from inherent optical properties on autonomous assets and remote sensing retrievals has made it possible to estimate C_{phyto} on large spatiotemporal scales (Behrenfeld et al., 2005). Further advances in the form of in situ calibration of C_{phyto} measurements have enhanced confidence in the parameter (Graff et al., 2015). However, due to logistical constraints and limited validation efforts, C_{phyto} algorithms substantially vary in accuracy and are regionally dependent (Martinez-Vincente et al., 2013; Serra-Pompei et al., 2023). Specifically, the Graff et al. (2015) C_{phyto} algorithm was developed using in situ samples from open-ocean regions of the North and South Atlantic and appears to be less accurate in regions with large phytoplankton standing stocks and higher concentrations of detrital and mineral particles, such as coastal, upwelling, and high latitude areas, including the Southern Ocean continental shelves. Accurate estimates of phytoplankton carbon are critical in the latter, given its substantial role in carbon cycling and the importance of the biological pump in that system (Le Quere et al., 2007; Gruber et al., 2019).

Analyses of how well the algorithm performs in various regions of the Southern Ocean have been conducted (Thomalla et al., 2019 and references therein), but applications of the algorithm to specific regions of the Southern Ocean have not been completed. The Ross Sea, which is responsible for approximately 28% of Southern Ocean net primary production (Arrigo et al., 2008), is of particular importance to carbon dynamics. It is the most productive shelf region of the Southern Ocean (Smith et al., 2014) and experiences an annual spring phytoplankton productive period where surface POC concentrations exceed 400 mg C m^{-3} and Chl *a* concentrations can be >15 µg L^{-1} ; Smith et al., 2000, 2011; Meyer et al., 2022). During the productive period, the phytoplankton assemblage is dominated initially by colonies of the haptophyte *Phaeocystis antarctica* before transitioning to dominance by a mixed assemblage of diatoms (Smith et al., 2000, 2011). This region also supports a substantial amount of macrofaunal biodiversity, with 38% of the world's Adelie penguins, 25% of the world's emperor penguins, 70% of Antarctic petrels, and an abundance of marine mammals (seals and whales; Ainley et al., 2015). However, studies on the non-algal organic carbon dynamics in this region are lacking, leading to uncertainties in our understanding of food web dynamics and carbon transformations.

II. Methods

We compiled POC-b_{bp}(470) calibration samples from three glider surveys in the Ross Sea. All gliders were launched from the fast ice near Ross Island and recovered by the *RVIB N.B. Palmer*. During glider recoveries CTD casts were completed as close to the glider dive location as possible, and water samples collected from known depths for POC and chlorophyll *a* calibration of the glider sensors. Kongsberg (formerly iRobot) Seagliders were deployed in 2010-2011, 2012-2012, and 2022-2023 during austral spring/summer (Fig. 1). POC-b_{bp}(470) samples were measured by an Imagenex 853 Echo Sounder and counts were

converted to POC concentrations following Boss and Pegau (2001). POC samples were processed according to Gardner et al. (2000). The Seagliders were also equipped with a Wet Labs ECO Triplet Puck to measure in situ fluorescence. Fluorescence was converted to Chl *a* concentrations according to Kaufman et al. (2014) and calibrated against samples which were analyzed fluorometrically on a Trilogy fluorometer (JGOFS, 1996). Full information on POC samples and processing and glider deployments are provided in Kaufman et al. (2014) and Meyer et al. (2022). All figures were made in Matlab (R2022b; The Mathworks, Inc.).

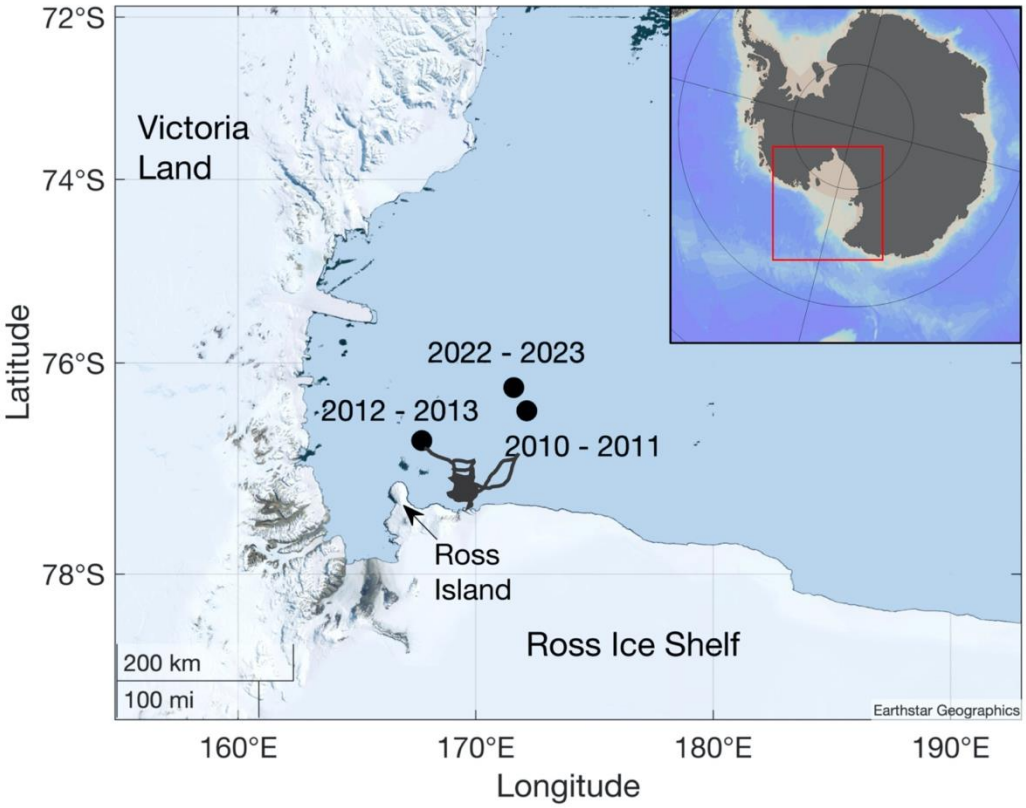

Figure 1. Map of calibration cast locations from the three glider deployments used in this study. Glider tracks from the 2012-2013 deployment are indicated in gray. All glider deployments occurred in the Ross Sea as indicated by the inset map.

Because C_{phyto} has not been measured directly in the Ross Sea, we used our $b_{bp}(470)$-based POC concentrations (concentrations (n = 29) ranged from 17.0 – 577 µg C L^{-1}), assuming 95% algal carbon in the surface waters during the annual bloom. We chose 95% as

our assumption after a sensitivity analysis was performed for assumptions of 40, 85, and 100% algal POC with 95% yielding the most realistic results. POC:Chl *a* ratios vs. depth for all three deployments showed no substantial decline with depth. Therefore, we applied our 95% algal carbon assumption uniformly through depth to all calibration samples. The data were then plotted, mimicking Graff et al. (2015), thus generating an equation for a C_{phyto} algorithm. We applied this algorithm to all three glider deployments, calculating C_{phyto} at 5 m. The 2012-2013 deployment was chosen as our case study to validate this regional tuning, given that it has been analyzed in the greater detail relative to the 2010-2011 and 2022-2023 studies (Jones and Smith, 2017; Meyer et al., 2022). In addition to C_{phyto}, the ratio of C_{phyto} to optically derived POC and fluorometrically derived Chl *a* (Jones and Smith, 2017; Kaufman et al., 2014) were calculated. All C_{phyto} concentrations and ratios were confined to the mixed layer to make them more closely comparable to satellite retrievals.

III. Results

Our calibration algorithm relating $b_{bp}(470)$ (m^{-1}) counts to C_{phyto} concentrations (µg L^{-1}) was (Supplemental Fig. S1):

$$C_{phyto} = 39474 * b_{bp}(470) + 46.1 \qquad (3)$$

where 39474 is the slope of the linear relationship between the glider backscatter ($b_{bp}(470)$) and the in situ POC modified to account for non-algal POC and 46.1 is the y-intercept. Average C_{phyto} concentrations for each glider deployment varied among the three deployments, and each had substantial variability within each data set (Table 1). For all three datasets, derived C_{phyto} concentrations were strongly correlated with POC concentrations (r^2 = 0.50, 0.96, 1.00, respectively). In 2012-2013, C_{phyto} increased from early to mid-December with increased variability in late January to early February; maximum values occurred on January 18th (Fig. 2a). The variability in C_{phyto} concentrations was small (mean = 84.2 ± 11.0

157 µg C L^{-1}; range from 63.0 – 150.0 µg C L^{-1}), whereas surface POC concentrations averaged

158 264 ± 81.4 µg C L^{-1} (104 to 756 µg C L^{-1}). The integrated mixed layer C_{phyto} was 3.52 ± 2.17

159 g C m^{-2} (Fig. 2b). However, due to substantial mixed layer variability, values were highly

160 variable, ranging from 0.67 – 13.9 g C m^{-2} in the 2012-2013 study (Fig. 2b; for details on

161 mixed layer depth calculations, see Meyer et al., 2022).

162

163 **Table 1. Surface (5 m) average, standard deviation, minimum, and maximum C_{phyto}**
164 **concentrations (µg C L^{-1}) from three Ross Sea glider deployments.**
165
166

Year	Average C_{phyto} (µg C L^{-1})	Minimum C_{phyto} (µg C L^{-1})	Maximum C_{phyto} (µg C L^{-1})
2010-2011	75.6 ± 17.8	37.4	281
2012-2013	84.1 ± 11.0	63.0	150
2022-2023	77.1 ± 14.2	57.8	123

180 All calculations use $b_{bp}470$ data applied to the algorithm from this study.
181

182

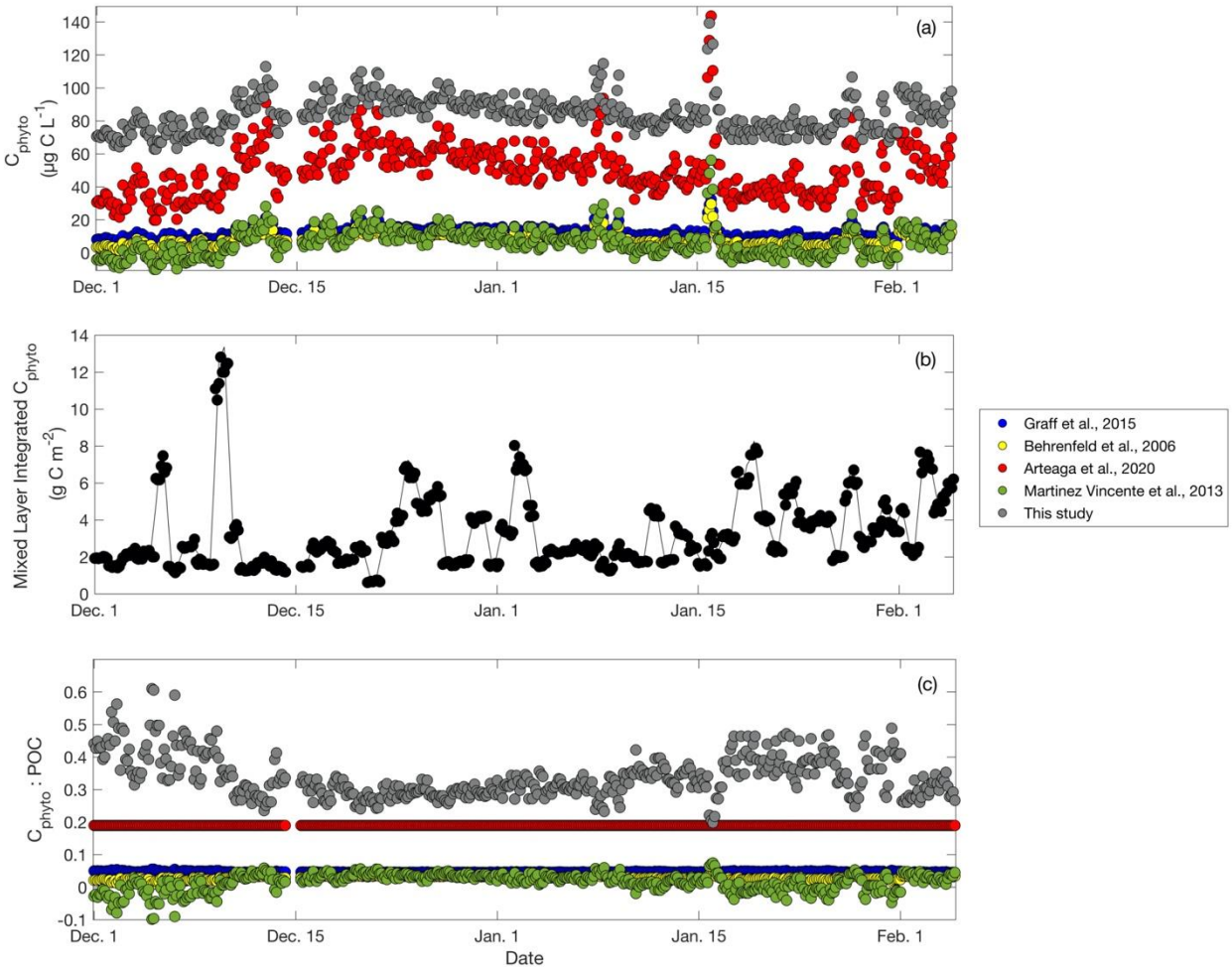

183

184 **Figure 2.** a) Surface (5 m) C_{phyto} concentrations from this study and previously published
185 algorithms, b) mixed layer integrated C_{phyto} concentrations calculated according to this
186 study's algorithm, and c) ratios of surface C_{phyto}:POC concentrations from this study and
187 previously published algorithms. All values are discrete and based on the 2012-2013
188 Seaglider deployment to the Ross Sea (Jones and Smith, 2017; Meyer et al., 2022). The black
189 line in b represents a 5-point running average of the data.
190

191 C_{phyto} concentrations were lower than anticipated, as exemplified by the ratios of
192 C_{phyto}:POC, which averaged 0.34 ± 0.07 over the survey period (Fig. 2c). However, our ratios
193 are within reported C_{phyto}:POC ratios (Behrenfeld et al., 2006), ranging from 0.20 – 0.61 and
194 are substantially higher than those calculated from any previously published algorithm (Fig.
195 2c). Patterns of C_{phyto}:POC ratios exhibited a different pattern from that of C_{phyto}
196 concentrations (Figs. 2c, 3a). Ratios declined in early to late December before increasing

slightly from early January through late January, and by early February, ratios begin to again decline, perhaps due to enhanced viral lysis or bacterial remineralization following increases in phytoplankton biomass. Because C_{phyto} concentrations remained consistent with those observed in mid-December through early January, this would suggest detrital carbon (i.e., POC – C_{phyto}) increased in mid- to late January, coincident with the highest concentrations of

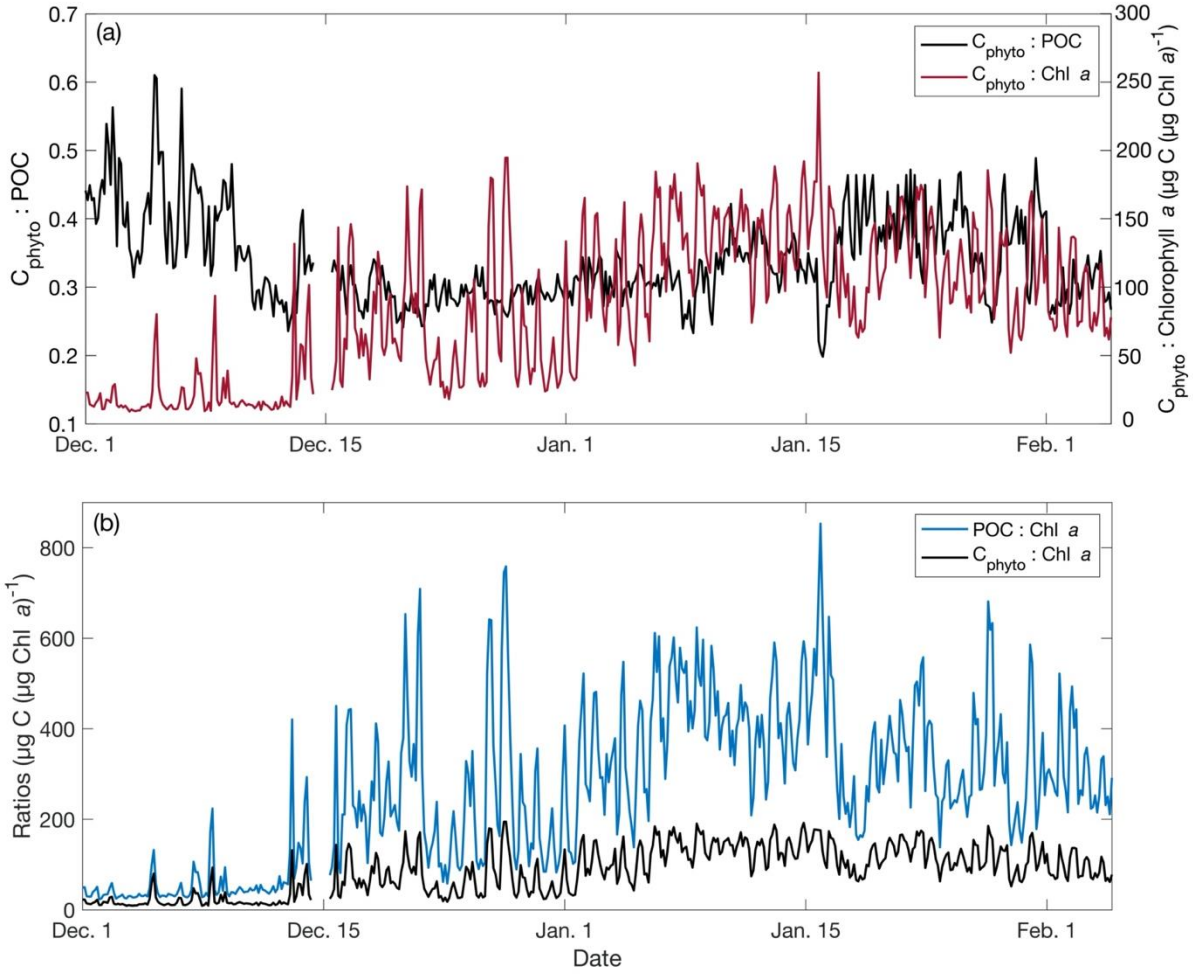

POC and the highest rates of net community production (Meyer et al., 2022).

Figure 3. Surface (5 m) ratios of (a) C_{phyto}:POC and C_{phyto}:Chl *a* concentrations (µg C (µg Chl *a*)$^{-1}$) and C_{phyto}:Chl *a* and POC:Chl *a* (µg C (µg Chl *a*)$^{-1}$) from the 2012-2013 Seaglider deployment to the Ross Sea.

Ratios of C_{phyto}:Chl *a* exhibit the same general pattern as POC:Chl *a* ratios (Meyer et al., 2022), averaging 85.3 ± 53.3 (average POC:Chl *a* ratios were 266 ± 179; Fig. 3b). While

the patterns remain consistent, the difference between C_{phyto}:Chl *a* and POC:Chl *a* can give further indication of phytoplankton physiology by providing a more specific relative cellular Chl content per unit carbon for *P. antarctica* vs. diatoms, i.e., the C_{phyto}:Chl *a* ratio is more comparable (differences between C_{phyto}:Chl *a* and POC:Chl *a* ratios range ~ < 70 – 564 µg C L^{-1}) in magnitude to POC:Chl *a* ratios during the period known to be dominated by diatoms (early January to early February) than during the period known to be dominated by *P. antarctica* (differences range 13 – 906 µg C L^{-1}; early to late December; Figs. 3a,b). While both exhibit large ranges, this would suggest that diatoms contribute more algal carbon to total POC than *P. antarctica*, likely due to a higher overall cellular POC to Chl *a* content as seen through the difference in C_{phyto}:Chl *a* and POC:Chl *a* ratios.

The greatest degree of uncertainty in these estimates results from the assumption that during the peak productive period 95% of the POC in the surface ocean is algal as well as limited calibration samples. While average C_{phyto} concentrations for the variety of assumptions tested are within previously reported estimates, ranging 30.3 to 170 µg C L^{-1} (Table 1; Table S1), given the lack of in situ C_{phyto} samples for validation and the relatively few number of calibration samples, we suspect our values are low. Another source of uncertainty results from sampling and analysis biases that come from POC samples and sensor precision. Early (2010-2011 and 2012-2013) calibration efforts collected single POC samples, but the 2022-2023 study collected duplicate POC samples with a standard deviation of 16.1 µg C L^{-1}. Additionally, the relatively few calibration samples and the highly dynamic environment always presents some uncertainty associated with the Echo Sounder (r^2 between bbp470 and in situ POC samples were 0.85, 0.80, and 0.63, for 2010-2011, 2012-2013, and 2022-2023, respectively).

IV. Discussion

Our C_{phyto} concentrations appear to be more accurate than those generated when applying global algorithms, lending confidence in the ability to regionally tune pre-existing algorithms to achieve a more realistic estimate of algal carbon. Our C_{phyto} concentrations and C_{phyto}:POC ratios are all greater than values calculated from previously reported algorithms (Figs. 2a, 3). The substantial difference between our calculated C_{phyto} concentrations and POC concentrations, as represented by a low (<50) average C_{phyto}:POC ratio in 2012-2013 (Arrigo et al., 2000, 2003; Meyer et al., 2022), is surprising and would suggest that C_{phyto} is still too low and is being limited by the lack of in situ data. Despite this, the C_{phyto}:POC ratios are within the range previously reported by Graff et al. (2015) and Burt et al. (2018) for other regions. C_{phyto}:POC ratios from the 2022-2023 deployment lend confidence to the method, producing higher but less variable values ranging from 0.50 to 0.53 (average = 0.51 ± 0.01), as 2022-2023 appeared to be more productive and with greater biomass relative to 2012-2013, supporting the notion of a higher C_{phyto} concentration. Interestingly, C_{phyto}:POC ratios from the 2010-2011 deployment were all >1. This year had low POC concentrations (mean mixed layer concentration < 110 µg C L^{-1}; Kaufman et al., 2014), as well as the weakest r^2 value between C_{phyto} and POC, suggesting our algorithm is better tuned to higher POC concentrations which are more characteristic of the Ross Sea during a typical productive period. However, given concentrations calculated by our algorithm for all years are higher than concentrations calculated by algorithms from other studies, it suggests our algorithm provides more realistic estimates for this region.

When applied to $b_{bp}(470)$ data from the Ross Sea, current global algorithms underestimate C_{phyto} substantially (by approximately >80%; Table 2). This is evident from extremely low C_{phyto}:POC ratios through the productive period (Table 2). The one exception to this is the Chl-derived method of Sathyendranath et al. (2009) which overestimates C_{phyto} concentrations substantially (average C_{phyto}:POC ratios > 3). C_{phyto}:POC is useful to evaluate

the proportion of algal relative to total carbon concentrations in the surface ocean. Whereas ratios of C_{phyto}:Chl *a* (µg C L^{-1}:µg Chl *a* L^{-1}) can be used to broadly assess the phytoplankton assemblage through pre-established relationships (Arrigo et al., 2000; Riemann et al., 1989) and assessments of spatio-temporal transitions (Figs. 4a,b). Our algorithm produced C_{phyto}:Chl *a* ratios within previously reported values (Kauffman et al., 2014; Smith and Kauffman, 2018), ranging from 9.01 in early December to >200 by mid-January.

Table 2. Previously published algorithms for optically derived phytoplankton-specific carbon (C_{phyto}).

Reference	Algorithm	C_{phyto} (µg C L^{-1})	C_{phyto}: POC
Behrenfeld et al., 2005	$C_{phyto} = 13000 * (b_{bp}(470) - 3.5x10^{-4})$	8.00	0.03
Sathyendranath et al., 2009	$C_{phyto} = 119 * (chl^{0.55})$	851	3.62
Martinez-Vincente et al., 2013	$C_{phyto} = 30100 * (b_{bp}(470) - 7.6x10^{-4})$	6.19	0.02
Graff et al., 2015	$C_{phyto} = 12129 * b_{bp}(470) + 0.59$	12.3	0.05
Arteaga et al., 2020	$C_{phyto} = 0.19 * POC$	50.1	0.19
This study	$C_{phyto} = 39474 * b_{bp}(470) + 46.13$	84.1	0.34

Algorithms, concentrations of C_{phyto}, and the ratio of C_{phyto} : particulate organic carbon (POC) as calculated from a Ross Sea glider deployment when sed algorithms are applied to this backscatter, chlorophyll *a* (chl), or POC datasets.

Despite the strong correlation between C_{phyto} and POC in our analysis, temporal patterns in the ratio of C_{phyto}:POC can provide more information on the algal vs. non-algal partitioning in the surface waters during the seasonal progression of the annual productive period (Fig. 3a). The patterns of C_{phyto}:POC appears largely driven by the higher variability in

POC concentrations rather than C_{phyto}, i.e., ratios are highest when POC concentrations are low in early December and lowest in late December when surface biomass is maximal (Figs. 3, 4a). The low degree of variability in ratios and C_{phyto} concentrations is noteworthy, given the substantial variability in POC concentrations themselves (standard deviation for surface POC = 81.3 µg C L^{-1}; Meyer et al., 2022). C_{phyto}:POC ratios increase slightly but significantly ($p < 0.05$) in late January - early February when bacterial remineralization has been hypothesized to increase and could change the concentration of the detrital carbon pool (Ducklow et al., 2001; Meyer et al., 2022). Whether this change results from a net decline in POC concentrations or increased detrital carbon is impossible to tell, but studies which capture the full decline in the productive period and final diatom reduction would resolve this.

One advantage of calculating C_{phyto} relative to either POC or Chl *a* is the removal of apparent changes in biomass related to physiological effects, such as irradiance impacts on fluorescence (Chl *a*), and environmental effects, such as a high concentration of non-algal carbon (POC). Changes in C_{phyto} concentrations reflect actual biomass changes and therefore, should exhibit a different temporal trend from both POC and Chl *a*. C_{phyto} should be more similar to POC, peaking later than Chl *a* in early to mid-January with a faster decline than POC. We hypothesize that POC concentrations would remain more elevated into mid- to late January than C_{phyto} because POC concentrations would likely be influenced by detrital POC resulting from processes like sloppy feeding (Steinberg et al., 2008), bacterial remineralization (Asper and Smith, 2019), and the generation of *Phaeocystis* ghost colonies (Smith et al., 2017), all of which may increase the non-algal POC pool. Additionally, trends in C_{phyto} can be compared to trends in nonphotochemical quenching (NPQ; Ryan-Keogh and Smith, 2021) that would impact Chl *a* concentrations. Like POC, C_{phyto} exhibited similar temporal patterns to NPQ, suggesting both are impacted by light and iron availability, but

303 that NPQ is not serving as a strong negative control on C_{phyto} concentrations themselves
304 (Ryan-Keogh and Smith, 2021).

305 The phytoplankton assemblage experiences a predictable shift from being dominated
306 by *P. antarctica* to being diatom dominated in mid-December to early January (Smith et al.,
307 2014; Meyer et al., 2022) - a pattern further confirmed by the increase in C_{phyto}:Chl *a* ratios.
308 The varying degrees of difference in POC:Chl *a* and C_{phyto}:Chl *a* during periods of *P.*
309 *antarctica* or diatom dominance would suggest that diatoms have less Chl *a* relative to
310 cellular carbon than *Phaeocystis* (Fig. 3b). This notion is further supported by the
311 discrepancy in patterns between C_{phyto}:POC and C_{phyto}:Chl *a* in early December where the
312 greatest difference corresponds to the period of *Phaeocystis* dominance (Fig. 3a). These
313 findings have implications for both remote sensing and carbon export dynamics and further
314 supports the argument for C_{phyto} as a proxy for phytoplankton biomass in biogeochemical
315 models. Application of this algorithm to additional datasets may help elucidate physical
316 factors that impact the balance between algal and non-algal carbon (Arrigo et al., 2003). How
317 this impacts food web dynamics and the transfer of organic carbon to higher trophic levels is
318 uncertain but warrants further investigation.
319

320 **V. Conclusion**

321 We developed a locally-tuned Ross Sea C_{phyto}-b_{bp} algorithm through in situ calibration
322 POC samples and sensor measurements and knowledge of the region's bloom dynamics. Our
323 analysis provides the most realistic constraint of C_{phyto} in this region to date. However, C_{phyto}
324 concentrations in the surface appear low relative to what we would expect given extensive
325 sampling in the Ross Sea. The accuracy of any C_{phyto} algorithm will be limited until in situ
326 validation to generate direct C_{phyto} estimates is conducted. Further initiatives toward this goal
327 and the overall development of regional algorithms are needed and would greatly improve

biogeochemical models of the region and our understanding of the mechanisms driving its role in carbon fluxes (Le Quere et al., 2007; Casey et al., 2013).

Data Availability

All data presented here are publicly available at the Biological and Chemical Oceanography Data Management Office (Woods Hole, MA; Smith, 2014; Smith, 2015) and at the British Oceanographic Data Centre (Southampton, UK; Heywood, 2023).

Funding

This work was supported by National Science Foundation grant ANT-2040571 to W. Smith and Natural Environment Research Council grant NE/W00755X/1 to K. Heywood.

Acknowledgements

We thank Danny Kaufman, Randy Jones for their work generating the original datasets for the calibration samples and Esther Portela, Karen Heywood, and the UEA Glider group for piloting the gliders in the 2022-2023 deployment. We also thank the captains and crews of the *RV/IB Nathaniel B. Palmer* during each of the glider recovery cruises.

References

Ainley, D.G., Ballard, G., Jones, R.M., Jongsomjit, D., Pierce, S.D., Smith, W.O., Jr., & Veloz, S. (2015). Trophic cascades in the western Ross Sea, Antarctica: revisited. *Marine Ecology Progress Series, 534*, 1-16. https://doi:10.3354/meps11394

Arrigo, K.R., DiTullio, G.R., Dunbar, R.B., Robinson, D.H., Van Woert, M., Worthen, D.L., & Lizotte, M.P. (2000). Phytoplankton taxonomic variability in nutrient utilization and primary production in the Ross Sea. *Journal of Geophysical Research, 105*, 8827–46.

354 Arrigo, K.R., Robinson, D.H., Dunbar, R.B., Leventer, A.R., & Lizotte, M.P. (2003).
355 Physical control of chlorophyll a, POC, and TPN distributions in the pack ice of the
356 Ross Sea, Antarctica. *Journal of Geophysical Research, 108.*
357 https://doi.org/10.1029/2001JC001138
358 Arrigo, K.R., van Dijken, G.L., & Bushinsky, S. (2008). Primary production in the Southern
359 Ocean, 1997–2006. *Journal of Geophysical Research, 113,* C08004.
360 https://doi.org/10.1029/2007JC004551.
361 Asper, V., & Smith, W.O., Jr. (2019). Variations in the abundance and distribution of
362 aggregates in the Ross Sea, Antarctica. *Elementa Science of the Anthropocene, 7,* 23.
363 https://doi.org/10.1525/elementa.355
364 Behrenfeld, M. J., Boss, E., Siegel, D. A., & Shea, D. M. (2005). Carbon based ocean
365 productivity and phytoplankton physiology from space. *Global Biogeochemical*
366 *Cycles, 19,* GB1006. https://doi:10.1029/2004GB002299
367 Boss, E., & Pegau, W.S. (2001). Relationship of light scattering at an angle in the backward
368 direction to the backscattering coefficient. *Applied Optics, 40,* 5503–5507.
369 https://doi.org/10.1364/AO.40.005503
370 Carlson, C.A., Hansell, D.A., Peltzer, E.T., & Smith, W.O., Jr. (2000). Stocks ad dynamics of
371 dissolved and particulate organic matter in the southern Ross Sea, Antarctica. *Deep-*
372 *Sea Research II, 47,* 3201–3225. https://doi.org/10.1016/S0967-0645(00)00065-5
373 Casey, J.R., Aucan, J.P., Goldberg, S.R., & Lomas, M.W. (2013). Changes in partitioning of
374 carbon amongst photosynthetic pico- and nano-plankton groups in the Sargasso Sea in
375 response to changes in the North Atlantic Oscillation. *Deep-Sea Research II, 93,* 58-
376 70. http://dx.doi.org/10.1016/j.dsr2.2013.02.002
377 Ducklow, H., Carlson, C., Church, M., Kirchman, D., Smith, D., & Steward, G. (2001). The
378 seasonal development of the bacterioplankton bloom in the Ross Sea, Antarctica,

1994-1997. *Deep-Sea Research II, 48,* 4199–4221. https://doi.org/10.1016/S0967-0645(01)00086-8

Gardner, W.D., Richardson, M.J., & Smith, W.O., Jr. (2000). Seasonal patterns of water column particulate organic carbon and fluxes in the Ross Sea, Antarctica. *Deep-Sea Research II, 47,* 3424–3449. https://doi.org/10.1016/S0967-0645(00)00074-6

Graff, J.R., Westberry, T.K., Milligan, A.J., Brown, M.B., Dall'Olmo, G., van Dongen Vogels, V., et al. (2015). Analytical phytoplankton carbon measurement spanning diverse ecosystems. *Deep Sea Research I, 102,* 16–25. https://doi:10.1016/j.dsr.2015.04.006

Gruber, N., Landschützer, P., & Lovenduski, N.S. (2019). The variable Southern Ocean carbon sink. *Annual Review of Marine Science, 11,* 159–186. https://doi.org/10.1146/annurev-marine-121916-063407

Heywood, K. (2023) Data from Predators to Plankton. British Oceanographic Data Centre (BODC). (Version 1) https://gliders.bodc.ac.uk/inventory/metadata-viewer/?DeploymentId=596 [accessed 11/20/2023]

Jones, R.M., & Smith, W.O., Jr. (2017). The influence of short-term events on the hydrographic and biological structure of the southwestern Ross Sea. *Journal of Marine Systems, 166,* 184–195. https://doi.org/10.1016/j.jmarsys.2016.09.006

Kaufman, D.E., Friedrichs, M.A.M., Smith, W.O., Jr., Queste, B.Y., & Heywood, K.J. (2014). Biogeochemical variability in the southern Ross Sea as observed by a glider deployment. *Deep-Sea Research I, 92,* 93–106. https://doi.org/10.1016/j.dsr.2014.06.011

Le Quere, C., Rodenbeck, C., Buitenhuis, E T., Conway, T.J., Langenfelds, R., Gomez, A., et al. (2007). Saturation of the Southern Ocean CO_2 sink due to recent climate change. *Science, 316,* 1735–1738. https://doi.org/10.1126/science.1136188

Martinez-Vicente, V., Dall'Olmo, G., Tarran, G., Boss, E., & Sathyendranath, S. (2013). Optical backscattering is correlated with phytoplankton carbon across the Atlantic Ocean. *Geophysical Research Letters, 40,* 1154–1158. https://doi.org/10.1002/grl.50252

Meyer, M.G., Jones, R.M., & Smith, W.O., Jr. (2022). Quantifying seasonal particulate organic carbon concentrations and export potential in the southwestern Ross Sea using autonomous gliders. *Journal of Geophysical Research, 127,* e2022JC018798. https://doi.org/10.1029/2022JC018798

Riemann, B., Simonsen, P., & Stensgaard, L. (1989). The carbon and chlorophyll content of phytoplankton from various nutrient regimes. *Journal of Plankton Research, 11,* 1037-1045.

Ryan-Keogh, T., & Smith, W.O., Jr. (2021). Temporal patterns of iron limitation in the Ross Sea as determined from chlorophyll fluorescence. *Journal of Marine Systems, 215,* 103500. https://doi.org/10.1016/j.jmarsys.2020.103500

Sathyendranath, S., Stuart, V., Nair, A., Oka, K., Nakane, T., Bouman, H., et al. (2009). Carbon-to-chlorophyll ratio and growth rate of phytoplankton in the sea. *Marine Ecology Progress Series, 383,* 73–84. https://doi:10.3354/meps07998

Serra-Pompei, C., Hickman, A., Britten, G.L., & Dutkiewicz, S. (2023). Assessing the potential of backscattering as a proxy for phytoplankton carbon biomass. *Global Biogeochemical Cycles, 37*. https://doi.org/10.1029/2022GB007556

Smith, W.O., Jr. (2014) Data from GOVARS iRobot Seaglider AUV-SG-502 released into McMurdo Sound, Southern Ross Sea, 2010-2011 (GOVARS project). Biological and Chemical Oceanography Data Management Office (BCO-DMO). (Version 1) Version Date 2014-10-08. https://lod.bco-dmo.org/dataset/532608 [accessed 11/15/2023]

Smith, W.O., Jr. (2015) Glider data from the southern Ross Sea collected from the iRobot Seaglider during the RVIB Nathaniel B. Palmer (AUV-SG-503-2012, NBP1210) cruises in 2012 (Penguin Glider project). Biological and Chemical Oceanography Data Management Office (BCO-DMO). (Version 4) Version Date 2015-12-09. http://lod.bco-dmo.org/id/dataset/568868 [accessed 04/04/2023]

Smith, W.O., Jr., Ainley, D.G., Arrigo, K.R., & Dinniman, M.S. (2014). The oceanography and ecology of the Ross Sea. *Annual Review of Marine Science, 6*, 469–487. https://doi.org/10.1146/annurev-marine-010213-135114

Smith, W.O., Jr., & Kaufman, D.E. (2018). Climatological temporal and spatial distributions of nutrients and particulate matter in the Ross Sea. *Progress in Oceanography, 168*, 182–195. https://doi.org/10.1016/j.pocean.2018.10.003

Smith, W.O., Jr., Marra, J., Hiscock, M.R., & Barber, R.T. (2000). The seasonal cycle of phytoplankton biomass and primary productivity in the Ross Sea, Antarctica. *Deep-Sea Research II, 47*, 3119-3140. https://doi.org/10.1016/S0967-0645(00)00061-8

Smith, W.O., Jr, Shields, A.R., Dreyer, J., Peloquin, J.A., & Asper V. (2011) Interannual variability in vertical export in the Ross Sea: magnitude, composition, and environmental correlates. *Deep-Sea Research I, 58*, 147−159.

Steinberg, D.K., Van Mooy, B.A.S., Buesseler, K.O., Boyd, P.W., Kobari, T., & Karl, D.M. (2008). Bacterial vs. zooplankton control of sinking particle flux in the ocean's twilight zone. *Limnology and Oceanography, 53*, 1327–1338. https://doi.org/10.4319/lo.2008.53.4.1327

The MathWorks, Inc. (2022). MATLAB version: 9.13.0 (R2022b). Accessed: December 13, 2023. Available: https://www.mathworks.com

Thomalla, S.J., Ogunkoya A.G., Vichi M., & Swart S. (2017) Using optical sensors on gliders to estimate phytoplankton carbon concentrations and chlorophyll-to-carbon

ratios in the Southern Ocean. *Frontiers in Marine Science, 4*, 34.
https://doi:10.3389/fmars.2017.00034